

Influence of NH₃/CO₂ Modification on the Characteristic of Biochar and the CO₂ Capture

Zhang Xiong · Zhang Shihong · Yang Haiping · Shi Tao ·
Chen Yingquan · Chen Hanping

Published online: 5 February 2013
© Springer Science+Business Media New York 2013

Abstract This paper was aimed to study the influence of modification of biochar on the performance of CO₂ adsorption. Biochar, obtained from cotton stalk pyrolysis in a fixed bed reactor, was modified with ammonia and CO₂. The physicochemical properties of biochars were characterized by the Fourier transform infrared spectroscopy and automatic adsorption equipment (Micromeritics, ASAP 2020, USA). CO₂ adsorption of biochar was performed in thermogravimetric analyzer. The results showed that the surface area of char was increased significantly by CO₂ modification, while N-contained compound on char surface was enriched obviously by NH₃ modification. CO₂ adsorption of biochar increased greatly with CO₂ and NH₃ modification. CO₂ adsorption was mainly attributed to physical adsorption at 20 °C, and the adsorption quantity (maximum = 99 mg/g) was proportional to the micropore volume of the char. However, at 120 °C, molecular thermal motion increase, chemical adsorption start to play a dominated role, and the adsorption was directly proportional to the N content of this char.

Keywords Biomass char · CO₂ activation · NH₃ modification · CO₂ adsorptions

Introduction

Carbon dioxide is the main greenhouse gas; the average concentration of CO₂ in the atmosphere is increasing at a

rate of 1.5 % per year [1]. Therefore, the reduction of CO₂ emission has become a critical issue. CO₂ capture and storage is a major technology to reduce CO₂ emission [2–4]. Among various CO₂ capture technologies, adsorption is a well-developed technology used in many industrial applications. However, respected to CO₂ adsorption, it is necessary to produce easily regenerable and durable adsorbents with a high CO₂ adsorption capacity [5–8]. Activated carbons attracted increasing concern as it is cheap, less sensitive to moisture, has high CO₂ adsorption capacity at ambient pressure, and the last but not the least it is easy to regenerate [9, 10].

Cotton stalks are a low-cost, relatively abundant agricultural waste, which can be used as a feedstock for the production of activated carbons enriched with the micropore through carbonization followed by activation with CO₂ [11, 12]. Some researchers believe that the micropore of the adsorbent plays an important role in CO₂ adsorption [4, 5, 8]. However, the adsorption properties of the adsorbent are primarily determined by its micropore structure as well as surface chemistry [13, 14]. Moreover, in the case of high temperature adsorption, the acid gases adsorption of activated carbon is strongly influenced by the surface chemistry [4, 10, 15, 16]. Adib et al. and Bagreev et al. have reported that the presence of nitrogen functionalities on the carbon surface could be conducive to the adsorption of acid gases, such as H₂S and SO₂ [15, 16]. It has been recognized that the introduction of basic nitrogen functionalities into the carbon surface can enhance the CO₂ adsorption capacity of the adsorbent. [2, 4, 17–21]. Reaction with gaseous ammonia is one of the suggested methods to introduce nitrogen into carbon matrix [22–28]. At high temperature, ammonia breaks down into some radicals, such as NH₂, NH, and H, and these radicals can react with surface oxides and active

Z. Xiong · Z. Shihong · Y. Haiping (✉) · S. Tao · C. Yingquan ·
C. Hanping
State Key Laboratory of Coal Combustion, Huazhong University
of Science and Technology, Wuhan 430074, China
e-mail: yhp2002@163.com

sites present at the edges of the graphene layers to form amines, amides, imides, lactams, nitriles, or pyridine- or pyrrole-like functionalities [26–30]. However the utilization of biochar as adsorbent for CO₂ capture was rarely reported. Accordingly, in this study, the property of CO₂ adsorption of biochar resulted from biomass pyrolysis was investigated, and with the influence of carbon dioxide and gaseous ammonia, modification was analyzed systematically.

Materials and Method

Sample

Cotton stalks collected locally were adopted as raw materials, and the proximate analyses and ultimate analyses were shown in Table 1. It can be seen that cotton stalk did not only have high volatile content, but also a certain amount of fixed carbon, so it was a good thermal energy resources for the pyrolysis bio-oil, char, and other products. Biochar resulted from cotton pyrolysis at 600 °C in N₂ atmosphere; the physicochemical properties of the char were shown in Table 2. It can be inferred that the biochar had well-developed pore structure and enriched surface nitrogen content.

Experimental Method

The biochar resulted from cotton stalk pyrolysis modified with carbon dioxide and ammonia, respectively. The modification process could be described as follows. Biochar particles (~2 g) in a quartz reactor were treated in a vertical tube furnace. The char was heated up gradually to preset temperature (500–900 °C) with N₂ purging. When the required temperature was reached, N₂ was replaced by CO₂ or NH₃ modifying respectively. In comparison, a blank trial was performed with N₂ as background.

The physical property of modified biochars was analyzed with isothermal adsorption of carbon dioxide at 298 K (Micromeritics, ASAP 2020, USA). The micropore surface area (S_{mic}) and micropore volume (V_{mic}) at various temperatures were calculated with Dubinin–Radushkevich (DR) method [13, 31]. The ultimate analysis of biochar was measured with CHNS elementary analyzer (Vario Micro cube, Germany). The organic species, especially N-contained organic functional group was characterized using

Fourier transform infrared spectroscopy (FTIR; VERTEX 70, Bruker, Germany) [31].

CO₂ adsorption of biochar was performed in fixed bed with a thermogravimetric analyzer. The experimental procedure is illustrated as following. Firstly, about 10 mg of the adsorbent was placed in a small sample pan and heated up to 110 °C under pure N₂ flow (50 ml/min) and held isothermally for 1 h to remove the moisture and gases. Then, the temperature was decreased to 20 °C, purging gas was switched to pure CO₂ at the same flow rate and biochar particles was held isothermally at 20 °C for 1 h to achieve a complete saturation. The weight increase during this stage was considered as the CO₂-adsorbed amount for the sample at 20 °C. Afterward, the temperature was increased at a heating rate of 5 °C/min to 120 °C (as a typical temperature for power plant flue gases) and this temperature was maintained for 1 h. The weight change of the sorbents was monitored to evaluate the CO₂ adsorption capacity at higher temperature (120 °C) [31–33].

Results and Discussion

Textural Characterization

The pore structure and surface nitrogen content of the virgin char and the modified samples were shown in Table 2. It showed that the microspore surface area and pore volume of the modified biochar gradually increased, with the modified temperature rising. It might be attributed that higher temperature (>600 °C) is favorable for interior devolatilization. The specific surface area of the CO₂-modified char was maximized at 800 °C (610.04 m²/g) and reduced to 556.35 m²/g (at 900 °C) with temperature increasing further. That was because of the CO₂ hot corrosion of char surface at higher temperatures, which led to the embrittlement of the carbon skeleton and the collapse of the carbon skeleton and micropore overlapping, so the specific surface area decreased. Moreover, the surface area and pore volume of the CO₂-modified char was much higher than the unmodified biochar and NH₃-modified biochar. At high temperatures, CO₂ could react with C of the sample to form CO (the hot corrosion), which helped to create a richer pore structure and played a role in activation of its surface. This reaction is endothermic, which means the reaction is more favorable at higher temperatures.

Table 1 The proximate and ultimate analysis result of agricultural straws

Samples	Proximate analysis (ad, wt%)				Ultimate analysis (ad, wt%)					LHV/MJ/kg
	M	V	A	FC	C	H	N	S	O	
Cotton stalks	4.66	74.95	4.59	15.80	45.22	6.34	1.15	0.34	37.70	17.77

Table 2 Characterization of the virgin char and the modified samples

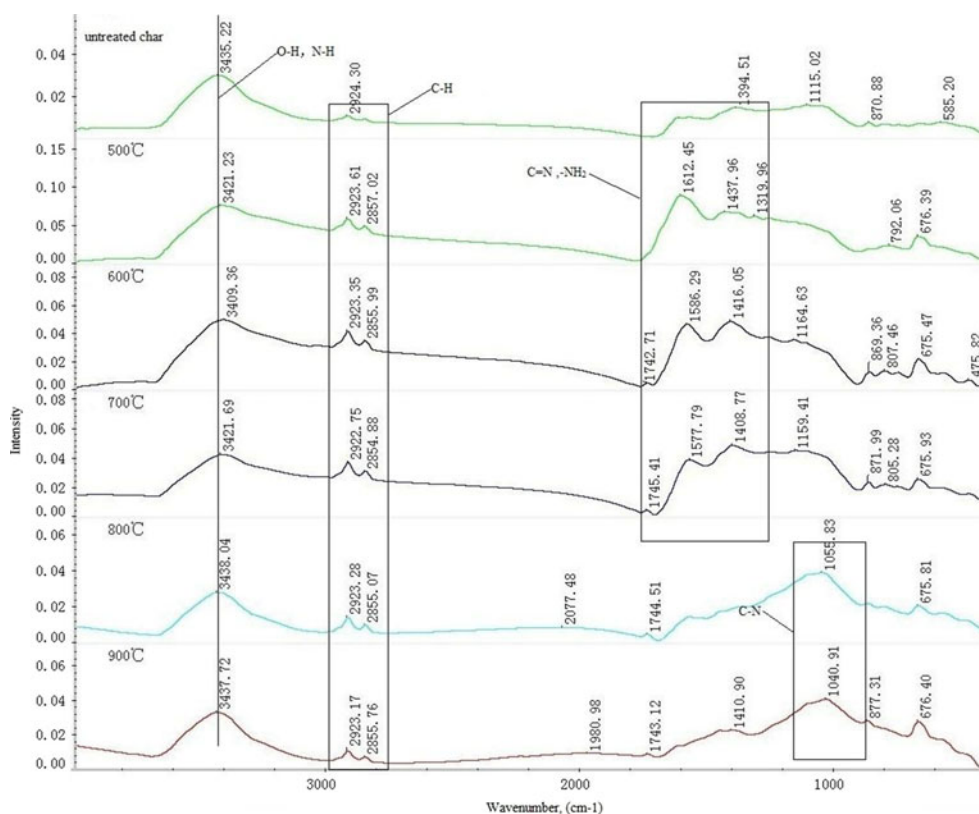
Modification temperature		500 °C	600 °C	700 °C	800 °C	900 °C
Biochar	Surface area of micropore (m ² /g)		224.12			
	Pore volume of micropore(ml/g)		0.07			
	Nitrogen content(wt%)		1.09			
NH ₃	Surface area of micropore (m ² /g)	160.89	251.91	254.97	348.56	434.92
	Pore volume of micropore(ml/g)	0.06	0.08	0.14	0.17	0.19
	Nitrogen content(wt%)	2.91	3.48	2.45	1.61	0.71
CO ₂	Surface area of micropore (m ² /g)	289.07	351.49	371.65	610.04	556.35
	Pore volume of micropore(ml/g)	0.12	0.13	0.14	0.24	0.21
	Nitrogen content(wt%)	1.28	1.02	0.78	0.54	0.47

Chemical Characterization

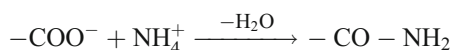
To study the nature of the functional groups of the modified and unmodified char, FTIR analysis was carried out. The FTIR spectra of the virgin char and NH₃-modified char were depicted in Fig.1; peaks were observed at 2,924 and 2,857 cm⁻¹ which could be attributed to asymmetric and symmetric C–H stretching vibrations in aliphatic CH, CH₂, and CH₃ [34]. The two other bands at 1,394 and 1,115 cm⁻¹ were due to aromatic ring and C–O stretch of ethers, respectively [33]. There was an obvious peak from the stretching of the N–H group and O–H group at 3,427~3,409 cm⁻¹, possibly due to the formation of hydrogen bonds between the NH₃ molecules with oxygen-containing groups of the

char [35, 36]. A broad band at 2,850 ~ 2,950 cm⁻¹ was due to the C–H groups [34]. A tiny peak at 1,742 cm⁻¹ was observed, which was a sign of carboxylic acid functional group, but as the temperature increased, the adsorption peak gradually disappeared [14, 37, 38]. An obvious broadband at 1,612 ~ 1,319 cm⁻¹ arising from the amides, pyridine, and C=N showed the introduction of nitrogen functional groups in the high temperature and NH₃ atmosphere compared to the unmodified biochar [33]. Perhaps because ammonia breaks down into some radicals, such as NH₂, NH, and H, at the temperature, and these radicals can react with surface oxides and active sites to form nitrogen-containing functional groups [18–23].

Fig. 1 Fourier transform infrared spectroscopy (the biochar and NH₃-modified biochar)



The lactam functional group was generated by the dehydration of the carboxylate (active sites of the carboxylic acid interacted with NH_3), at high temperatures:



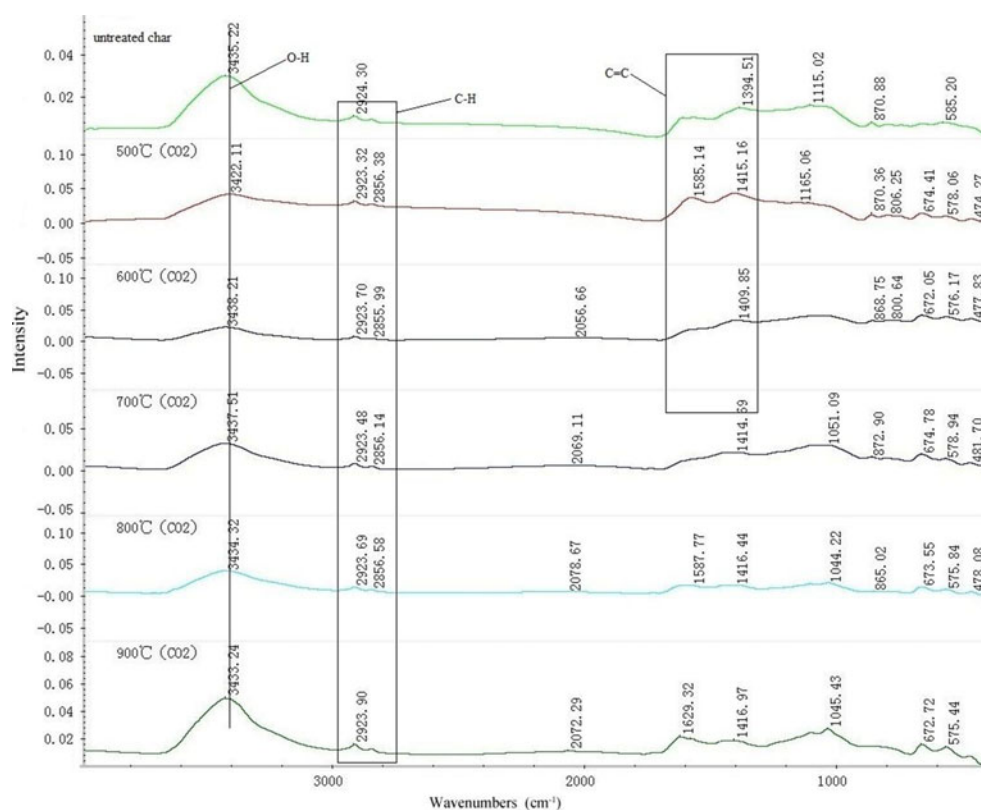
In addition, at high temperatures, NH_3 and O–H were also easy to generate $-\text{NH}_2$ (amide):



The adsorption peak (at $1,609 \sim 1,584 \text{ cm}^{-1}$) was caused by the aromatic conjugated $\text{C}=\text{C}$ and $\text{C}=\text{N}$ functional group [39]. With the increase of modification temperature increasing, the $\text{C}=\text{N}$ and amide decomposed; the adsorption peak diminished gradually and shifted to $1,437 \sim 1,159 \text{ cm}^{-1}$, owing to the formation of the $\text{C}-\text{N}-\text{C}$ or pyridine substances [14, 21, 37, 38]. Shafeeyan et al. found that the original double bond of the nitrogen-containing functional groups shifted to a more stable single bond or a ring structure, with increasing temperature [38].

The pyridine was not only from the amide decomposition, but also from the $-\text{NH}-$ alternative ethers functional groups [28, 30]. A broadband at $1,040 \sim 1,055 \text{ cm}^{-1}$ was due to the $\text{C}-\text{N}$ group [4, 22, 40]. Above $800 \text{ }^\circ\text{C}$, on the one hand, the $\text{C}=\text{C}$ and NH_3 reacted to form a new nitrogen-containing functional groups ($\text{C}-\text{N}$); on the other hand, the $\text{C}=\text{N}$ bond was ruptured to $\text{C}-\text{N}$ bond [14, 22, 41].

Fig. 2 Fourier transform infrared spectroscopy (the biochar and CO_2 -modified biochar)



On the contrary, the CO_2 -modified biochar contained O–H, $\text{C}-\text{C}$, $\text{C}-\text{H}$, and other functional groups, but the N functional groups did not appear (as shown in Fig. 2). In addition, the adsorption curve at $1,400 \sim 1,750 \text{ cm}^{-1}$ leveled off because the modified char had the good pore structure in the CO_2 atmosphere at the price of the gradual consumption about $\text{C}-\text{H}$ and $\text{C}-\text{O}$ bonds, but it had not introduced the new N functional groups [33, 40]. However, there is a tiny adsorption peak at $1,585 \sim 1,415 \text{ cm}^{-1}$ that gradually disappeared, with the rise in temperature. This reason may be the aromatic $\text{C}=\text{C}$ bond breaking.

The N element content of the NH_3 -modified biochar was much higher than that of the unmodified biochar and CO_2 -modified biochar (shown in Table 2). This showed that at high modification temperature, NH_3 reacted with the sample and successfully introduced nitrogen-containing functional groups to improve the alkalinity of the biochar. However, the N element content of the NH_3 -modified biochar decreased sharply with the increase temperature. This might be because some nitrogen-containing functional groups decomposed at higher temperature ($900 \text{ }^\circ\text{C}$); consequently, nitrogen content in NH_3 -modified biochar decreased slightly with modified temperature increasing further.

Properties of CO_2 Adsorption

The adsorption capacity of the CO_2 -modified char and unmodified char are showed in Fig. 3. At ambient temperature,

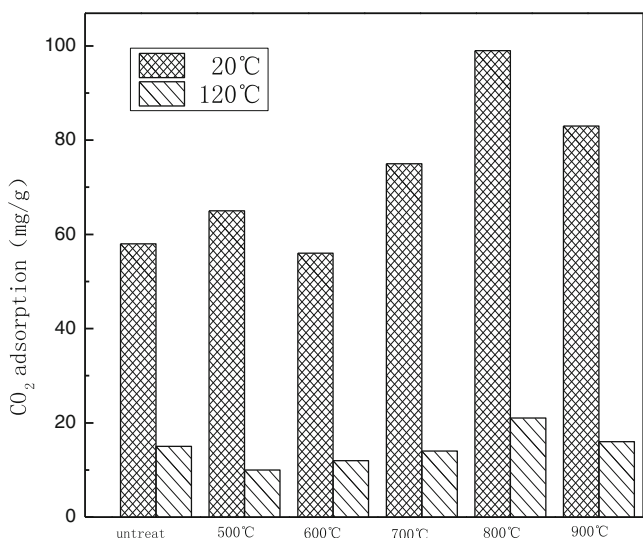


Fig. 3 The adsorption capacity of the CO₂-modified char

the adsorption capacity of the CO₂-modified char is significantly higher than that of the char without CO₂ modification. Especially, when the modifying temperature was higher than 700 °C, the adsorption capacity of the CO₂-modified char could reach 90–100 mg/g (at 20 °C). This shows that the CO₂ atmosphere was conducive to the formation of the char’s pore structure at higher temperature; consequently, it is favorable for CO₂ adsorption at ambient temperature. Figure 4 shows the adsorption capacity of the NH₃-modified char and unmodified char. At ambient temperature, the adsorption volume of the NH₃-modified char (the modified temperature between 500 and 700 °C) are clearly less than the untreated char. That may be due to the introduction of N-contained materials that led some

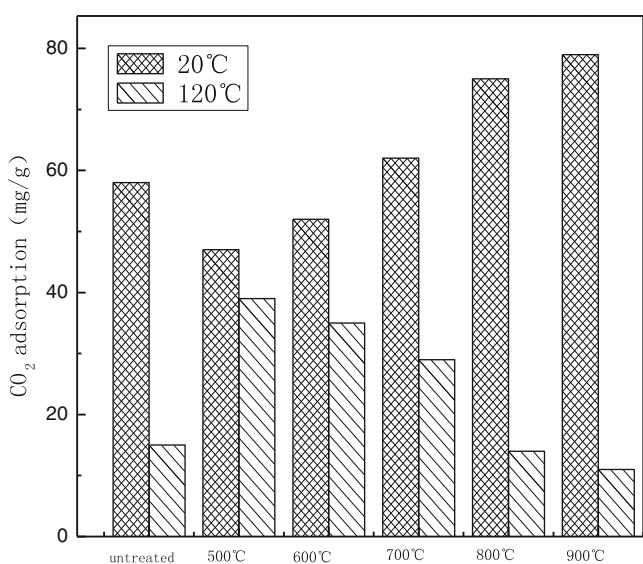


Fig. 4 The adsorption capacity of the NH₃-modified char

micropores clogging [21], but when the temperature increases (>700 °C), the amount of adsorption will be increased, and more than the untreated char. It may be because that some functional groups decompose and micropores open again [4, 9, 21].

However, at 120 °C, the NH₃-modified char showed higher CO₂ adsorption capacity (about 39 mg/g) compared with the unmodified char (less than 20 mg/g) and the CO₂-modified char (about 20 mg/g). Moreover, when the modified temperature was between 500 and 700 °C, the high temperature adsorption (at 120 °C) of the NH₃-modified chars is greatly higher than that of the CO₂-modified chars and untreated char. This shows that the introduction of the N functional groups by the NH₃ modification, at high temperatures, does contribute to the CO₂ adsorption capacity of the modified biochar [25, 33]. Nevertheless, at the modified temperature of 800 and 900 °C, although NH₃-modified chars have high nitrogen content, their high temperature adsorption are obviously less than that of the CO₂-modified chars. It may be because of their poor microporous structure and beneficial nitrogen functional groups of decomposition at high temperature [33–35, 40].

The Fig. 5 and Fig. 6 showed the relationship between the CO₂ adsorption capacity of the modified char and the micropore volume and nitrogen content. At 20 °C, the adsorption capacity showed linear relationship with the micropore volume and CO₂ adsorption increased straightly with the increase of micropore volume. However, no obvious relation showed with N content, it is mainly physical adsorption, and adsorbed

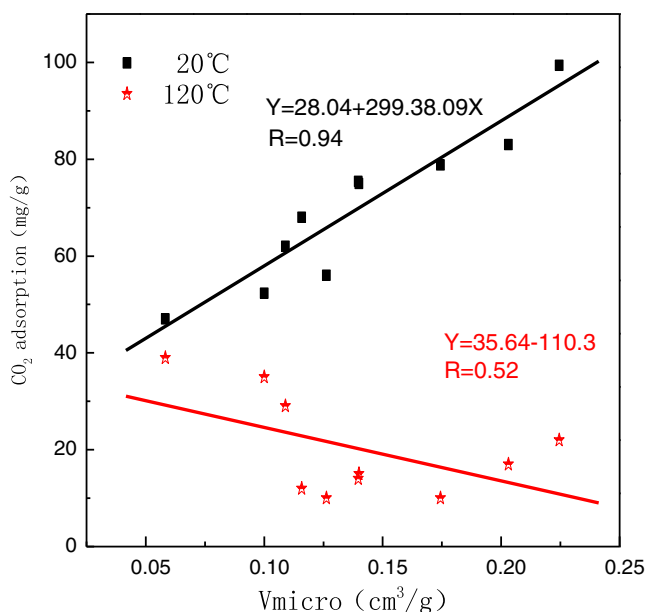


Fig. 5 The relationship between the CO₂ adsorption capacity of the modified char and the micropore volume

in pore. The correlation equation of adsorption with micropore volume can be described by the DR equation [42].

$$V = V_0 \exp \left[- \left(\frac{RT}{\beta E} \ln \frac{P_s}{P} \right)^2 \right] \quad (1)$$

Where V_0 is the volume adsorbed at a relative pressure of P_s/P and temperature T , V is the micropore volume, E is the energy of adsorption, β is the affinity coefficient of the adsorbate, and R is the universal gas constant. This equation can be written as

$$\log V = \log V_0 + K \times \log^2(P_s/P) \quad (2)$$

$$K = -(RT/\beta E)^2 \quad (3)$$

To enhance the adsorption property of char at ambient temperature, modification to open pore structure might be a good alternative. However, at 120 °C, no obvious relationship showed between CO₂ adsorption capacity and the micropore volume. But it showed closed relationship with the nitrogen content in char particles, and CO₂ adsorption increased linearly with N content. It indicated that the adsorption at higher temperature is mainly chemical adsorption by N-contained compounds. Surface chemistry characteristics might be the main factor to control the CO₂ adsorption at higher temperature. Thus, for CO₂ capture at higher temperature with biochar, chemical modification with N-contained materials might be a promising choice.

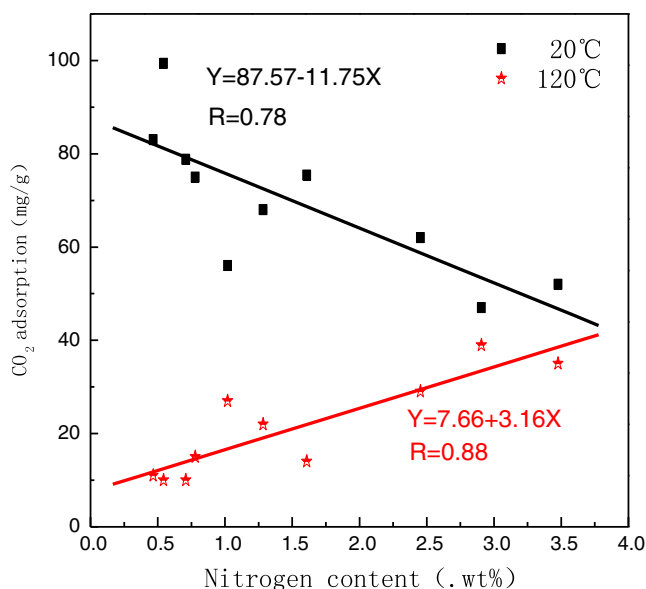


Fig. 6 The relationship between the CO₂ adsorption capacity of the modified char and the nitrogen content

Conclusions

The property of biochar modification with CO₂ activation and NH₃ was investigated with the aim to enhance the CO₂ adsorption. The main conclusion can be derived as follows:

1. For ammonia-modified char, NH₃ could react with the biochar surface, introducing the nitrogen functional groups, but the nitrogen functional groups with increasing temperature would gradually break down. CO₂ modification play significant role on pore formation, and more micropore was formed with CO₂ activation and the maximum surface area was reached at 800 °C,
2. The lower the temperature, the greater the high-temperature adsorption capacity of the NH₃-modified biochar, but the low-temperature adsorption capacity was similar to the CO₂-modified biochar. At room temperature, the largest CO₂ adsorption capacity of the NH₃-modified biochar was 99 mg/g; however, it was 39 mg/g at 120 °C.
3. At ambient temperature, the CO₂ adsorption of the modified biochar was mainly physical adsorption, and it was a linear correlation with the micropore volume. But at higher temperature, the adsorption was a chemical adsorption, and a linear relationship with the N content on the char surface.

Acknowledgments The author wishes to express her sincere thanks to the financial support from National Natural Science Foundation of China (51276075 and 51021065) and National Key Technology R&D Program in the 12th Five-Year Plan of China (2011BAD15B05-03).

References

1. Brunner G (2009) Near critical and supercritical water, Part I. Hydrolytic and hydrothermal processes. *J Supercrit Fluids* 47 (3):373–381
2. Drage TC, Arenillas A, Smith KM, Pevida C, Piippo S, Snape CE (2007) Preparation of carbon dioxide adsorbents from the chemical activation of urea–formaldehyde and melamine–formaldehyde resins. *Fuel* 86(1):22–31
3. Li W, Choi S, Drese JH, Hornbostel M, Krishnan G, Eisenberger PM, Jones CW (2010) Steam-stripping for regeneration of supported amine-based CO₂ adsorbents. *Chem Sus Chem* 3(8):899–903
4. Plaza M, Pevida C, Arenillas A, Rubiera F, Pis J (2007) CO₂ capture by adsorption with nitrogen enriched carbons. *Fuel* 86 (14):2204–2212
5. Arenillas A, Smith K, Drage T, Snape C (2005) CO₂ capture using some fly ash-derived carbon materials. *Fuel* 84(17):2204–2210
6. Liang Z, Marshall M, Chaffee AL (2009) CO₂ adsorption-based separation by metal organic framework (Cu-BTC) versus zeolite (13X). *Energy Fuel* 23(5):2785–2789
7. Plaza M, Pevida C, Arias B, Casal M, Martín C, Feroso J, Rubiera F, Pis J (2009) Different approaches for the development of low-cost CO₂ adsorbents. *J Environ Eng* 135(6):426–432

8. Xu X, Song C, Andresen JM, Miller BG, Scaroni AW (2002) Novel polyethylenimine-modified mesoporous molecular sieve of MCM-41 type as high-capacity adsorbent for CO₂ capture. *Energ Fuels* 16(6):1463–1469
9. Plaza M, Rubiera F, Pis J, Pevida C (2010) Ammoxidation of carbon materials for CO₂ capture. *Appl Surf Sci* 256(22):6843–6849
10. Yang RT (1986) Gas separation by adsorption processes. Butterworth, Stoneham
11. Rodriguez-Reinoso F, López-González JD, Berenguer C (1984) Activated carbons from almond shells—II: characterization of the pore structure. *Carbon* 22(1):13–18
12. Rodriguez-Reinoso F, Molina-Sabio M (1992) Activated carbons from lignocellulosic materials by chemical and/or physical activation: an overview. *Carbon* 30(7):1111–1118
13. Liu WJ, Zeng FX, Jiang H, Zhang XS (2011) Preparation of high adsorption capacity bio-chars from waste biomass. *Bioresour Technol* 102(17):8247–8252
14. Swiatkowski A, Pakula M, Biniak S, Walczyk M (2004) Influence of the surface chemistry of modified activated carbon on its electrochemical behaviour in the presence of lead(II) ions. *Carbon* 42(15):3057–3069
15. Bagreev A, Bashkova S, Bandosz TJ (2002) Adsorption of SO₂ on activated carbons: the effect of nitrogen functionality and pore sizes. *Langmuir* 18(4):1257–1264
16. Adib F, Bagreev A, Bandosz TJ (2000) Adsorption/oxidation of hydrogen sulfide on nitrogen-containing activated carbons. *Langmuir* 16(4):1980–1986
17. Maroto-Valer MM, Tang Z, Zhang Y (2005) CO₂ capture by activated and impregnated anthracites. *Fuel Process Technol* 86(14):1487–1502
18. Mercedes Maroto-Valer M, Lu Z, Zhang Y, Tang Z (2008) Sorbents for CO₂ capture from high carbon fly ashes. *Waste Manag* 28(11):2320–2328
19. Pevida C, Plaza M, Arias B, Feroso J, Rubiera F, Pis J (2008) Surface modification of activated carbons for CO₂ capture. *Appl Surf Sci* 254(22):7165–7172
20. Plaza M, Pevida C, Arias B, Feroso J, Arenillas A, Rubiera F, Pis J (2008) Application of thermogravimetric analysis to the evaluation of aminated solid sorbents for CO₂ capture. *J Therm Anal Calorim* 92(2):601–606
21. Przepiorski J, Skrodzewicz M, Morawski A (2004) High temperature ammonia treatment of activated carbon for enhancement of CO₂ adsorption. *Appl Surf Sci* 225(1):235–242
22. Biniak S, Szymański G, Siedlewski J, Świątkowski A (1997) The characterization of activated carbons with oxygen and nitrogen surface groups. *Carbon* 35(12):1799–1810
23. Bota KB, Abotsi GMK (1994) Ammonia: a reactive medium for catalysed coal gasification. *Fuel* 73(8):1354–1357
24. Boehm HP, Mair G, Stoehr T, De Rincón AR, Tereczki B (1984) Carbon as a catalyst in oxidation reactions and hydrogen halide elimination reactions. *Fuel* 63(8):1061–1063
25. Jansen R, Van Bekkum H (1994) Amination and ammoxidation of activated carbons. *Carbon* 32(8):1507–1516
26. Meldrum BJ, Rochester CH (1990) In situ infrared study of the surface oxidation of activated carbon in oxygen and carbon dioxide. *J Chem Soc Faraday Trans* 86(5):861–865
27. Vinke P, Van der Eijk M, Verbree M, Voskamp A, Van Bekkum H (1994) Modification of the surfaces of a gas activated carbon and a chemically activated carbon with nitric acid, hypochlorite, and ammonia. *Carbon* 32(4):675–686
28. Stöhr B, Boehm H, Schlögl R (1991) Enhancement of the catalytic activity of activated carbons in oxidation reactions by thermal treatment with ammonia or hydrogen cyanide and observation of a superoxide species as a possible intermediate. *Carbon* 29(6):707–720
29. Grant KA, Zhu Q, Thomas KM (1994) Nitrogen release in the gasification of carbons. *Carbon* 32(5):883–895
30. Jansen R, Van Bekkum H (1995) XPS of nitrogen-containing functional groups on activated carbon. *Carbon* 33(8):1021–1027
31. Chen Y, Wang X, Chen H, Yang H, Zhang S (2012) Biomass-based pyrolytic polygeneration system on cotton stalk pyrolysis: influence of temperature. *Bioresour Technol* 107:411–418
32. Plaza M, Pevida C, Arias B, Feroso J, Rubiera F, Pis J (2009) A comparison of two methods for producing CO₂ capture adsorbents. *Energy Procedia* 1(1):1107–1113
33. Shafeeyan MS, Daud WMAW, Houshmand A, Arami-Niya A (2011) Ammonia modification of activated carbon to enhance carbon dioxide adsorption: effect of pre-oxidation. *Appl Surf Sci* 257(9):3936–3942
34. Moreno-Castilla C, Ferro-García M, Joly J, Bautista-Toledo I, Carrasco-Marin F, Rivera-Utrilla J (1995) Activated carbon surface modifications by nitric acid, hydrogen peroxide, and ammonium peroxydisulfate treatments. *Langmuir* 11(11):4386–4392
35. Chen JP, Wu S (2004) Acid/base-treated activated carbons: characterization of functional groups and metal adsorptive properties. *Langmuir* 20(6):2233–2242
36. Pradhan BK, Sandle N (1999) Effect of different oxidizing agent treatments on the surface properties of activated carbons. *Carbon* 37(8):1323–1332
37. Plaza M, Pevida C, Martín C, Feroso J, Pis J, Rubiera F (2010) Developing almond shell-derived activated carbons as CO₂ adsorbents. *Sep Purif Technol* 71(1):102–106
38. Shafeeyan MS, Daud WMAW, Houshmand A, Shamiri A (2010) A review on surface modification of activated carbon for carbon dioxide adsorption. *J Anal Appl Pyrol* 89(2):143–151
39. Lazar G, Lazar I (2003) IR characterization of a-C:H:N films sputtered in Ar/CH₄/N₂ plasma. *J Non-Cryst Solids* 331(1):70–78
40. Mangun CL, Benak KR, Economy J, Foster KL (2001) Surface chemistry, pore sizes and adsorption properties of activated carbon fibers and precursors treated with ammonia. *Carbon* 39(12):1809–1820
41. Hontoria-Lucas C, Lopez-Peinado A, López-González JD, Rojas-Cervantes M, Martín-Aranda R (1995) Study of oxygen-containing groups in a series of graphite oxides: physical and chemical characterization. *Carbon* 33(11):1585–1592
42. Kapoor A, Ritter J, Yang R (1989) On the Dubinin–Radushkevich equation for adsorption in microporous solids in the Henry's law region. *Langmuir* 5(4):1118–1121